Journal of Medical Virology

WILEY

JOURNAL OF MEDICAL VIROLOGY

RESEARCH ARTICLE OPEN ACCESS

Modulation of Lymphotoxin β Surface Expression by Kaposi's Sarcoma-Associated Herpesvirus K3 Through Glycosylation Interference

Soowon Kang[1] | Kevin Brulois[2] | Youn Jung Choi[3] | Shaoyan Zhang[1] | Jae U. Jung[1]

[1]Department of Infection Biology, Global Center for Pathogen and Human Health Research, Lerner Research Institute, Cleveland Clinic, Cleveland, Ohio, USA | [2]Department of Molecular Microbiology and Immunology, Keck School of Medicine, University of Southern California, Los Angeles, California, USA | [3]Department of Medicine, Division of Rheumatology, Kao Autoimmunity Institute, Cedars-Sinai Medical Center, Los Angeles, California, USA

Correspondence: Jae U. Jung (JUNGJ@ccf.org)

Received: 7 October 2024 | **Revised:** 20 December 2024 | **Accepted:** 7 January 2025

Funding: This study was supported by grants from the US *National Institutes of Health (NIH)* CA251275, CA294881, AI152190, AI17120, AI181758, DE023926, DE028521, and U01 CA294881 (Jae U. Jung) and a gift from Sheikha Fatima bint Mubarak.

ABSTRACT

Kaposi's sarcoma-associated herpesvirus (KSHV) employs diverse mechanisms to subvert host immune responses, contributing to its infection and pathogenicity. As an immune evasion strategy, KSHV encodes the Membrane-Associated RING-CH (MARCH)-family E3 ligases, K3, and K5, which target and remove several immune regulators from the cell surface. In this study, we investigate the impact of K3 and K5 on lymphotoxin receptor (LTβR) ligands, LTβ and LIGHT, which are type II transmembrane proteins and function as pivotal immune mediators during virus infection. Upon co-expression of viral MARCH proteins with LTβR ligands, we showed that K3 and K5 selectively targeted LTβ, but not LIGHT, for the downregulation of surface expression. Specifically, K3 and K5 E3 ligases interacted with the transmembrane domain of LTβ. Intriguingly, K3 interacted with an immature form of LTβ, whereas K5 targeted the fully mature form. Subsequent biochemical analyses revealed that K3 disrupted the initial steps of N-glycosylation maturation of LTβ. This interference resulted in the sequestration of LTβ within the endoplasmic reticulum, impeding its trafficking to the plasma membrane. Consequently, the K3-mediated downregulation of LTβ surface expression suppressed the LTβR downstream signaling pathway. These findings uncover a novel mechanism by which KSHV K3 E3 ligase inhibits the membrane trafficking pathway of the LTβ inflammatory ligand through glycosylation interference, potentially evading LTβR-mediated antiviral immunity.

1 | Introduction

Kaposi's sarcoma-associated herpesvirus (KSHV), also known as human herpesvirus 8 (HHV-8), is a member of the Herpesviridae family and is implicated in the pathogenesis of several malignancies such as Kaposi's sarcoma (KS), primary effusion lymphoma (PEL), and multicentric Castleman's disease (MCD), particularly in immunocompromised individuals [1–3]. A hallmark of KSHV infection is its ability to establish a persistent, lifelong infection that remains typically asymptomatic in immunocompetent individuals, despite continuous monitoring by the innate and adaptive immune systems [4, 5]. This persistence is facilitated by the virus's sophisticated strategies to evade host immune responses, which are crucial for its survival and pathogenesis [6].

One of the key mechanisms by which KSHV manipulates the host immune system is by modulating processes occurring at the host cell membrane, including immune recognition, cell adhesion, and signal transduction. Several viral genes encoded

by KSHV play significant roles in altering the plasma membrane dynamics of host cells. For instance, the replication and transcription activator (RTA), encoded by ORF50, suppresses Toll-like receptor 3 (TLR3) and TLR4 signaling pathways by downregulating their adaptor proteins, TRIF and myeloid differentiation primary response protein 88 (MyD88), respectively [7, 8]. Additionally, RTA reduces the surface expression levels of TLR2 and TLR4 by mediating the downregulation of their protein expressions [9]. KSHV also encodes viral transmembrane (TM) proteins such as ORF74 (vGPCR), K1, and K15, which influence cell survival, signaling, and proliferation [10]. These proteins can activate multiple signaling pathways, acting as receptors that lead to increased production of cytokines, chemokines, and growth factors. This activation promotes cell proliferation, transformation, and survival, contributing to the pathogenesis of KSHV-associated diseases [11–20]. Furthermore, the viral proteins K3 and K5, also known as modulators of immune recognition 1 and 2 (MIR1 and MIR2), directly interact with immune regulators on the plasma membrane [21]. Both K3 and K5 target molecules such as MHC class I and CD1d, while K5 additionally targets B7-2, ICAM-1, PECAM-1, and DC-SIGN [22–27]. By reducing the surface expression of these critical immune molecules, K3 and K5 facilitate immune evasion, allowing the virus to persist within the host.

K3 and K5 share significant similarities and are classified as immediate early or early genes, playing roles in the early stages of viral infection [28–32]. They may also be expressed during latency in response to Notch signaling, indicating their involvement in both phases of the viral life cycle [33]. Both proteins contain a RING-CH-type zinc finger domain and belong to the Membrane-Associated RING-CH (MARCH) family of E3 ubiquitin ligases [34, 35]. The RING-CH domain is essential for their function, mediating the ubiquitination of target proteins on lysine, cysteine, serine, or threonine residues [34, 36–40]. This ubiquitination leads to the internalization and lysosomal degradation of the targeted proteins, altering the immune capabilities of the host cell mediated by membrane proteins.

A crucial aspect of the host's antiviral defense is the lymphotoxin β receptor (LTβR) signaling pathway, which involves two ligands: $LT\alpha_1\beta_2$ and LIGHT [41–43]. $LT\alpha_1\beta_2$ is a heterotrimeric protein composed of a soluble LTα subunit tethered to the TM protein LTβ, which serves as a ligand. LTβR signaling is critical for the rapid production of type I interferons (IFNs) in response to viral infections, functioning independently of conventional Toll-like receptor signaling systems. For example, human cytomegalovirus (HCMV), type of β-herpesvirus, can replicate in dermal fibroblasts by suppressing IFN induction. However, activation of LTβR signaling can override this suppression, inducing IFNs that protect surrounding cells from viral infection [44, 45]. In murine models, LTβR signaling has been shown to initiate the first wave of IFN production during mouse CMV infection, highlighting its role in preserving lymphoid organ integrity and initiating effective immune responses [46–48]. LTβR signaling also plays a significant role in regulating responses to RNA viruses, such as vesicular stomatitis virus (VSV). LTβR-differentiated macrophages capture VSV, facilitating viral replication and antigen presentation, which are crucial for adaptive immunity while preventing the selection of IFN-resistant viral mutants [49, 50]. These findings underscore the importance of the LTβR pathway as a critical source of early IFNs, essential for both innate and adaptive immune responses.

Given the pivotal role of LTβR signaling in antiviral immunity and KSHV's known strategies to evade immune detection, it is plausible that KSHV may target components of the LTβR pathway to facilitate its infection and persistence. Here, we demonstrate lymphotoxin β (LTβ), the TM protein that forms the $LT\alpha_1\beta_2$ complex and acts as a ligand for LTβR, as a novel target for the viral E3 ligase proteins KSHV K3 and K5. Our overexpression assays showed that both K3 and K5 significantly reduced LTβ surface expression through direct interaction. Beyond identifying a new cellular target for these viral E3 ligases, we also uncovered distinct regulatory mechanisms. KSHV K3 alters LTβ glycosylation and inhibits its trafficking to the plasma membrane in an E3 ligase function-dependent manner, leading to the sequestration of LTβ within the endoplasmic reticulum (ER). These findings suggest that KSHV K3 may suppress antiviral signaling responses by disrupting the $LT\alpha_1\beta_2$–LTβR signaling pathway.

2 | Materials and Methods

2.1 | Cells Lines and Cell Culture

HEK-293T and Hela cells were cultured in Dulbecco's modified Eagle's medium (DMEM, Gibco) supplemented with 10% fetal bovine serum (FBS, Gibco) and 1% penicillin/streptomycin (Gibco). THP-1 cells were cultured in DMEM (Gibco) supplemented with 10% FBS (Gibco), 1% penicillin/streptomycin (Gibco), and 1× β-mercaptoethanol (Gibco). BJAB cells were cultured in RPMI 1640 medium (Gibco) supplemented with 10% FBS and 1% penicillin/streptomycin. BJAB cells stably transfected with pIRES-EF1α-puro (BJAB-EV), pIRES-K3-puro (BJAB-K3), and pIRES-K5-puro (BJAB-K5), as previously described [51], were grown in complete BJAB culture media as described above, and additionally supplemented with 2 μg/mL puromycin. All cells were maintained at 37°C in a humidified incubator with 5% CO_2. Before the experiments, cell lines were tested with MycoAlert Mycoplasma Detection Kit (Lonza) and confirmed as mycoplasma negative.

2.2 | Plasmids Constructs

KSHV K3, K5, and mutants have been described in previous research [34, 52], and were transferred into pCDH-CMV-MCS-EF1α-CopGFP plasmid for flow cytometry assays. The pIRES-EF1α-K3-puro and pIRES-EF1α-K5-puro constructs are described previously. Genes encoding LTβ, LIGHT, and HLA-A2 (02:01) were cloned into the pIRES-EF1α-puro vector with a C-terminal (LTβ, LIGHT) or an N-terminal (HLA-A2) FLAG tag. The LTβ N222Q mutation was generated using the QuikChange II Site-directed mutagenesis kit (Agilent) with the pIRES-EF1α-LTβ-puro construct as a template. Full-length LTβ and its mutants were cloned into the pEBG construct to add N-terminal glutathione *S*-transferase (GST) tag. For imaging, the LTβ-T2A-LTα gene fragment was synthesized (IDT) and

cloned into pLV-EF1α-IRES-puro, and further inserted mScarlet-I sequences at the C-terminus of LTβ. The K3-miRFP670nano3 and K3mZn-miRFP670nano3 gene fragments were synthesized (IDT) and cloned into pLV-EF1α-IRES-hygro. The pLV-EF1a-IRES-puro and pLV-EF1a-IRES-Hygro were a gift from Tobias Meyer (Addgene #85134) [53].

2.3 | Materials and Inhibitors

Tunicamycin powder, a glycosylation inhibitor, was purchased from Sigma and dissolved in DMSO. 12-O-tetradecanoylphorbol-13-acetate (TPA) was purchased from Cell Signaling and dissolved in DMSO. Recombinant human LTβR/TNFRSF3 Fc chimera and recombinant human IgG1 Fc protein were purchased from R&D Systems.

2.4 | Flow Cytometry

For surface staining, cells were harvested and washed in Dulbecco's phosphate-buffered saline (DPBS, Gibco), containing 1% FBS. They were stained with the proper antibodies or isotype control, as indicated. Following fluorescent antibody incubations, the cells were fixed in 4% formaldehyde in DPBS, if needed. For intracellular staining, the Cytofix/Cytoperm Fixation/Permeabilization Kit (BD Biosciences) was used following manufacturer's instructions. Flow cytometry was performed on an BD FACS Celesta (BD Biosciences), followed by analysis using FlowJo v10.1 software (Tree Star Inc.). The following antibodies and isotype controls were used; PE anti-FLAG (BioLegend, 1:400), APC anti-FLAG (BioLegend, 1:200), PE anti-human LT-α (BioLegend, 1:100), Alexa Fluor 647 anti-pIKKα/β (Ser176/180) (Cell Signaling, 1:50), PE mouse IgG1κ isotype control (BioLegend), APC mouse IgG1κ Isotype control (BioLegend), Alexa Fluor 647 rabbit IgG isotype control (Cell Signaling), and FITC mouse IgG1κ isotype control (eBioscience).

2.5 | Immunoblotting

Cells were lysed in 1% Triton X-100 lysis buffer supplemented with protease inhibitor cocktail (Roche) right before lysis and quantified by BCA assay (Pierce). Equal amounts of protein extract were resolved on SDS-PAGE gels and transferred onto PVDF membranes. Transferred membranes were incubated with specific antibodies in 5% non-fat milk in TBS-T (Sigma) followed by HRP-conjugated secondary antibodies. Images were developed with ECL reagent (Cytiva Life Sciences) and imaged on a Bio-Rad ChemiDoc-Touch. The used antibody information and concentrations were as follows: anti-DYKDDDDK tag (MA1-91878, Sigma, 1:2000), anti-KSHV K3 (lab generated, 1:5000), anti-KSHV K5 (lab generated, 1:5000), anti-V5 tag (Thermo Fisher, 1:2000), anti-GST tag (Santa Cruz, 1:2000), anti-LANA (LN53, Millipore, 1:1000), anti-β-actin (Santa Cruz, 1:2000), anti-rabbit IgG HRP-linked antibody (Cell Signaling, 1:5000), anti-rat IgG HRP linked antibody (Santa Cruz, 1:5000), and anti-mouse IgG HRP-linked antibody (Cell Signaling, 1:5000).

2.6 | Co-Immunoprecipitation and GST-Pulldown

HEK293T cells were transfected with the indicated DNA plasmids using polyethylenimine transfection (Sigma). Cells were harvested 48 h post-transfection, washed by DPBS pH7.5 (Gibco), and re-suspended in 1% Triton X-100 lysis buffer containing 50 mM Tris-HCl pH8.0 (Invitrogen), 150 mM NaCl (Sigma), 1% Triton X-100 (Sigma), supplemented with a protease inhibitor cocktail (Roche) right before lysis. After freeze/thaw cycle, whole-cell lysates (WCLs) were incubated on the shaker at 4C for 1 h and centrifuged for 10 min at 12 000*g*. The supernatants were filtered through a 0.45 μm polyethersulfone (PES) filter. For co-immunoprecipitation, WCL were incubated with Pierce Protein A/G Agarose (Thermo Fisher) and indicated antibodies at 4°C for overnight. For GST-pulldown, WCL were incubated with glutathione-conjugated Sepharose beads (GE) at 4°C for 1 h. Incubated beads were washed five times using 1% Triton X-100 wash buffer containing 50 mM Tris-HCl pH8.0 (Invitrogen), 200-400 mM NaCl (Sigma), 1% Triton X-100 (Sigma). Beads were eluted in 2× Laemmli protein sample buffer (Sigma) by heating at 95°C for 5 min. Samples were centrifuged for 5 min at 12 000*g* and subjected to immunoblotting.

2.7 | Flow Cytometry-Based Protein Export Assay

BJAB-LTβ-FLAG stable cells were rinsed two times with DPBS and incubated with excess amount of polyclonal anti-FLAG antibody (Millipore, 1:10) on ice for 1 h to saturate LTβ on the cell surface. Cells were rinsed with cold DPBS twice and incubated at 37°C in a humidified incubator with 5% CO_2 for 0, 2, 4, or 6 h. After incubation, cells were immediately chilled on ice and stained with PE anti-FLAG (BioLegend, 1:200) for 30 min to label newly exported LTβ. Cells were fixed with 4% formaldehyde and kept at 4°C until all samples were ready. LTβ surface expression levels were measured by a BD FACS Celesta (BD Biosciences), followed by analysis using FlowJo v10.1 software (Tree Star Inc.).

2.8 | Pulse-Chase Assay

Pulse-Chase assay was performed as described previously [51]. Prior to the pulse, cells were rinsed three times with DPBS, washed once with starvation media (RPMI without methionine and cysteine plus 3% dialyzed FBS, 10 mM HEPES [pH 7.4], 1% L-glutamine) for 15 min, and then incubated with 5 mL of the same medium containing 100 μCi/mL of [^{35}S]methionine and [^{35}S]cysteine (New England Nuclear, Boston, Massachusetts) for 10 min. For chase analysis, the labeled cells were chased for 0, 15, 30, 60, and 90 min. For immunoprecipitation, cells were harvested and lysed with lysis buffer (1% Triton X-100 in TBS) containing phenylinethylsulfonyl fluoride (PMSF) and iodoacetate (IAA). Immunoprecipitation was performed with a 1:500-diluted anti-FLAG antibody (Sigma) together with 30 μL of protein A- and protein G-agarose beads. After binding with lysates and washing the beads, washed immunoprecipitated beads were resuspended in 20 μL of 50 mM sodium citrate (pH 5.5)—0.2% sodium dodecyl sulfate, heated for 5 min at 95°C, and incubated for 6 h at 37°C with or without endo-β-N-

acetylglucosaminidase H (endo H) as indicated in the figure and figure legend. Relative signal intensity was analyzed using ImageJ/Fiji.

2.9 | Confocal Microscopy

HeLa cells were seeded on coverslips in 24-well plates and then transfected with pLVpuro-LTβ-mScarlet-I-T2A-LTα and pLVhygro-K3-/K3mZn-miRFP670nano3. ER-selective staining was performed using the ER-ID green assay kit (Enzo Like Sciences) following manufacturer's protocol with cells fixed with 4% paraformaldehyde (Thermo Fisher). After ER-staining and fixation, coverslips were mounted on glass slides with Fluoromount-G Mounting Medium (SouthernBiotech). The images were acquired using an SP8 confocal microscope (Leica). Images from each channel were processed and analyzed using ImageJ/Fiji.

2.10 | Coculture Assay

To prepare signal donor cell, BJAB-EV and BJAB-K3 were activated for 48 h with 50 ng/mL TPA. After activation, the cells were washed twice and kept in Opti-MEM (Gibco) for 1 h on ice. For measuring LTβR signaling activation, THP-1 cells, as signal recipient cell, were cocultured with activated BJAB cells at a 1:1 ratio. After 16 h incubation, cocultured cells were washed 3 times and harvested for further experiments. To remove BJAB cells from the coculture mixture, cells were stained with PE mouse anti-CD19 antibody (BD Biosciences) and CD19-population was negatively selected using Anti-Mouse IgG MicroBeads (Miltenyi Biotec).

2.11 | Quantitative RT-PCR (qRT-PCR)

Total RNA was extracted using RNeasy Micro kit (Qiagen) and cDNA was reverse transcribed from 100 ng of total RNA using iScript Reverse Transcription Supermix (Bio-Rad) according to the manufacturer's instructions. qPCR was conducted using SsoAdvanced Universal SYBR Green Supermix (Bio-Rad) on a Bio-Rad CFX96 thermocycler. The qPCR primers used in this study are shown below; CCL19-F (5′-TGCCTGCTGTAG TGTTCACC-3′), CCL19-R (5′-GCAGTCTCTGGATGATGCG T-3′), CXCL12-F (5′-TGCCCTTCAGATTGTAGCC-3′), CXCL 12-R (5′-AGTCCTTTTTGGCTGTTGTGC-3′), GAPDH-F (5′-TG GGCTACACTGAGCACCAG-3′), and GAPDH-R (5′-GGGTGT CGCTGTTGAAGTCA-3′).

2.12 | KSHV Virus Preparation and Infection

KSHV WT and ΔK3 viruses were prepared from BAC16 WT or ΔK3 containing iSLK cells as previously described [54, 55]. Briefly, 70% confluent iSLK-BAC16 cells were induced with a growth medium containing 1 mM sodium butyrate (Sigma) and 1 μg/mL doxycycline (Sigma). Four days later, culture medium containing virus was harvested and cleared by centrifugation and filtering by 0.45 μm PES filter to remove cells and debris. Viruses were concentrated by ultracentrifugation for 3 h at 24 000 rpm in SW32 rotor (Beckman Coulter). Virus pellets were resuspended in DPBS and stored at −80°C. For de novo infection of KSHV, when target transfected HEK293T cells reached 60%–70% confluence, cells were incubated with KSHV for 4 h at 37°C and then the inoculum was removed following three times of washing with DPBS. The growth medium was added before being returned to the incubator. After 48 h incubation upon infection, cells were collected for further experiments.

2.13 | Quantification and Statistical Analysis

All data were analyzed with Prism software (v10.0.2, GraphPad) using Student's t test. Unless otherwise stated, all experiments were performed at least two times, and the data were combined for presentation as mean ± SEM. All differences not specifically indicated as significant were not significant (n.s., $p > 0.05$). Significant values were indicated as $*p < 0.05$; $**p < 0.01$; $***p < 0.001$; $****p < 0.0001$. Statistical parameters are described in the Figures and Figure Legends.

3 | Result

3.1 | KSHV K3 and K5 Downregulate Surface Expression of LTβ, Not LIGHT

Given that K3 and K5 interact with the TM domains of various target surface proteins, we investigated the effect of these viral proteins on LTβR ligands, LTβ and LIGHT. The well-known target of K3 and K5, HLA-A2, was included as a control to validate the functionality of these viral proteins. The surface expression level of LTβ markedly decreased following the expression of either K3 or K5, while the surface expression of LIGHT remained largely unchanged under the same conditions (Figure 1A). The downregulation effect was mostly abolished in the K3 mutant (K3mZn) and completely absent in the K5 mutant (K5mZn), both with defective RING-CH E3 ligase domain. The surface levels of HLA-A2 were effectively downregulated by both viral proteins as reported [51].

To further examine the effect of K3 and K5 on target expression, we examined the expression levels of LTβ, LIGHT, and HLA-A2 in WCLs following expression of K3, K5, or their mutants. We found that neither K3 nor K5 transient expression affected the total expression levels of LTβ, LIGHT and HLA-A2 (Figure 1B). Interestingly, a lower molecular weight form (LMW, ~29 kDa) of LTβ was observed only in cells expressing K3, but not in those expressing K3mZn, K5 or K5mZn (Figure 1B). In contrast, a higher molecular weight form (HMW, ~33 kDa) of LTβ remained at comparable levels upon expression of K3, K3mZn, K5 or K5mZn. Finally, neither the expression levels nor the molecular weights of LIGHT and HLA-A2 were affected by the expression of K3, K3mZn, K5 or K5mZn (Figure 1B). These results indicate that K3 expression induces both a reduction in the molecular weight and surface expression of LTβ in an E3 ligase enzymatic activity-dependent manner. These results indicate that the K3-mediated reduction in LTβ molecular

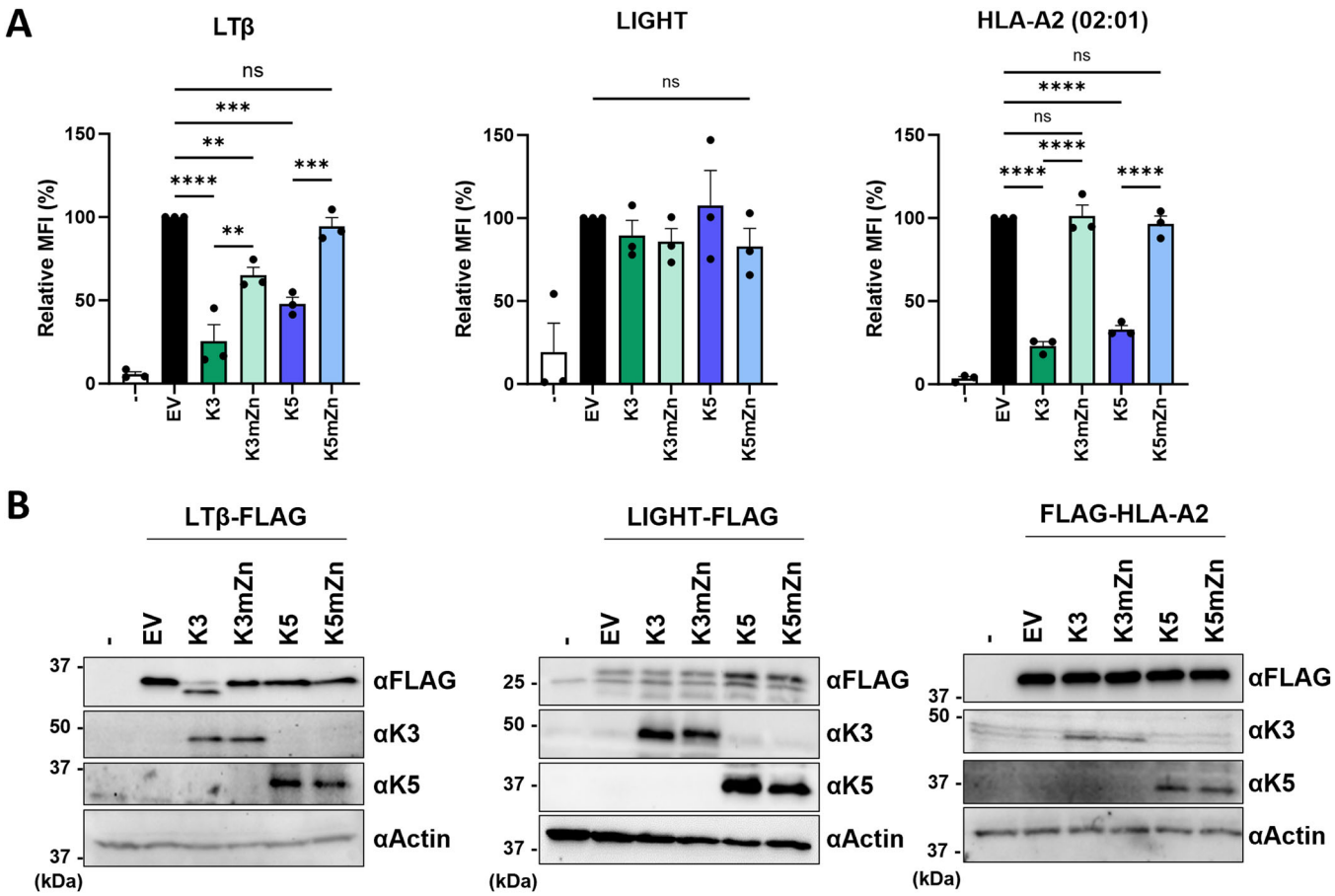

FIGURE 1 | KSHV E3 ligases can inhibit surface expression of LTβ, not LIGHT. (A) The HEK293T cells were co-transfected with wild-type or mutant KSHV E3 ligase (K3/K3mZn/K5/K5mZn) plasmid containing a copGFP reporter and target (LTβ-FLAG, LIGHT-FLAG, FLAG-HLA-A2) expressing plasmids as indicated at a 1:1 ratio (1 μg each). Forty-eight hours post-transfection, the surface expression levels of the targets were measured with anti-FLAG antibody from copGFP-positive population. The detailed gating strategy is described in Supporting Information S1: Figure S1A. Relative mean fluorescence intensity (MFI, %) of targets upon K3s or K5s expression were determined based on MFI of empty vector (EV). (B) A representative western blot data of cells described in (A). Error bars indicate SEM from triplicates. Statistical significance was calculated using an unpaired, two-tailed Student's *t* test. ns, not significant; $^{**}p < 0.01$; $^{***}p < 0.001$; $^{****}p < 0.0001$.

weight is strictly dependent on E3 ligase enzymatic activity, whereas the decrease in surface expression is largely, but not completely, influenced by this activity.

3.2 | KSHV K3 and K5 Interact With LTβ Through Its TM Domain

LTβ is a type II TM protein composed of an N-terminal cytoplasmic region, a TM, and a C-terminal TNF homology domain [56, 57]. A previous study demonstrated that direct interaction through the TM domain of the target is crucial for recognition by KSHV K3 and K5, and that the juxtamembrane domain of targets may also play a significant role in these interactions [58]. To investigate the potential interaction of KSHV K3 and K5 with LTβ, V5-tagged K3 or K5 was co-expressed with FLAG-tagged LTβ for immunoprecipitation. This showed a specific interaction of K3 or K5 with LTβ (Figure 2A). Notably, the LMW form of LTβ showed the efficient interaction with K3.

To further dissect this interaction, we generated GST fusion constructs of full-length LTβ and various mutants (Figure 2B). GST pulldown showed that GST fusions containing full-length LTβ, ΔTNF or ΔExtracellular mutants efficiently interacted with K3 or K5 (Figure 2C). In contrast, GST-LTβ Cyto-only mutant showed a loss of binding to K3 or K5 (Figure 2C). Notably, the GST-LTβ TM-only construct retained strong interactions with both K3 and K5 (Figure 2C). These results demonstrate that K3 and K5 interact with LTβ via its TM domain.

3.3 | KSHV K3 Alters LTβ Glycosylation in an E3 Ligase Activity-Dependent Manner

K3 expression induced both a reduction in the molecular weight and surface expression of LTβ in an E3 ligase enzymatic activity-dependent manner. Since LTβ contains a single N-glycosylation site (N222) on its extracellular domain [42, 59], we hypothesized that KSHV K3 reduces LTβ surface expression by impeding its glycosylation. To test this hypothesis, LTβ was co-expressed with K3 or its mutant variant K3mZn, following treatment with tunicamycin, a competitive inhibitor of N-acetylglucosamine phosphotransferase [60]. Upon tunicamycin treatment, the LMW form of LTβ was detected, similar to the effect observed

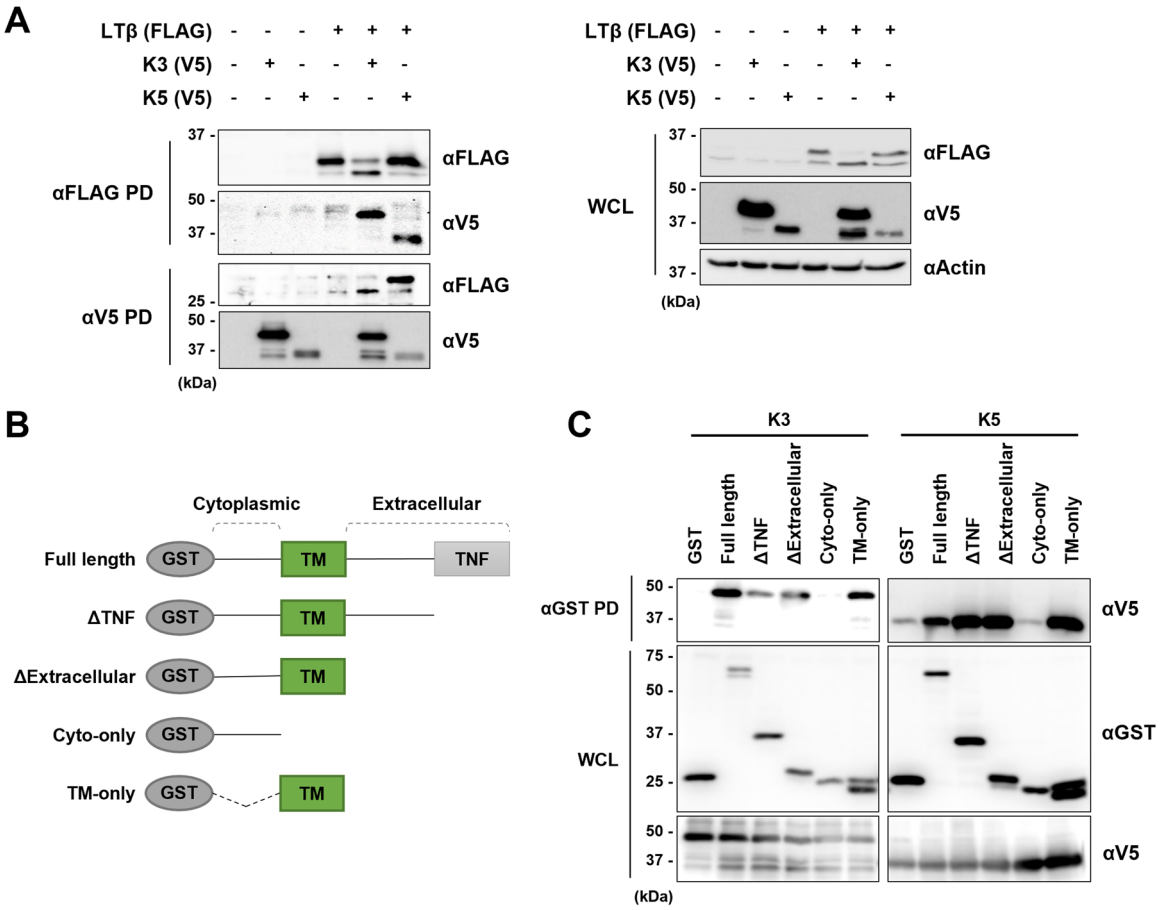

FIGURE 2 | KSHV E3 ligases directly interact with LTβ through its TM. (A) The HEK293T cells were co-transfected with V5-tagged K3 or K5 expressing plasmids and FLAG-tagged LTβ expressing plasmids as indicated at a 1:1 ratio (1 μg each). Forty-eight hours post-transfection, the whole-cell lysates (WCLs) were collected and performed pull-down (PD) assay with A/G beads with indicated antibodies, followed by immunoblotting. (B) Schematic overview of full-length and truncated mutant constructs for interacting assay with K3 and K5. (C) The HEK293T cells were co-transfected with V5-tagged K3 or K5 expressing plasmids and GST-tagged LTβ expressing plasmids as described in (B) at 1:1 ratio (1 μg each). Forty-eight hours post-transfection, the WCLs were collected and performed PD assay with glutathione-conjugated Sepharose beads, followed by immunoblotting. TM, transmembrane domain; TNF, tumor necrosis factor domain.

with the expression of WT K3, but not with the K3mZn mutant (Figure 3A). Notably, while K3 expression reduced the molecular weight of LTβ, it had no such effect on HLA-A2, which also contains an extracellular glycosylation site (Figure 1B). However, K3 downregulated the surface expression of both LTβ and HLA-A2.

To further test the effect of K3 on LTβ glycosylation, we used HEK293S GnTI$^-$ cells, which lack N-acetyl-glucosaminyl transferase I (GnTI) activity in the *cis*-Golgi, leading to the lack of complex N-glycans of glycoproteins [61]. In GnTI-deficient cells, the ratio of the two forms of LTβ expression was similar to that observed in GnTI-intact cells. The HMW form of LTβ remained dominant in HEK293S GnTI$^-$ cells expressing the empty vector (EV) or the K3mZn mutant, while the LMW form of LTβ was dramatically increased following WT K3 expression (Figure 3B). Since GnTI activity occurs later than tunicamycin's inhibition of glycosylation, this suggests that K3 disrupts the early stage of LTβ N-glycosylation, prior to the GnTI-effective phase. Collectively, these results indicate that KSHV K3 specifically hinders the early stages of LTβ N-glycosylation in an E3 ligase-dependent manner.

3.4 | Impaired Glycosylation of LTβ by KSHV K3 Hinders Its Transport to the Plasma Membrane

The glycosylation of surface membrane proteins is a crucial modification for proper folding, stability, and subcellular trafficking [62]. The N-glycosylation of LTβ at the N222 residue on its extracellular domain is essential for proper trafficking to the plasma membrane, particularly when forming a heterotrimer with LTα [57, 63, 64]. Consistently, the glycosylation-defective mutant N222Q of LTβ showed impaired surface expression (Figure 4A). To assess the impact of K3-mediated inhibition of LTβ glycosylation on its surface trafficking, we conducted flow cytometry-based protein export assay. Initially, we saturated the already expressed LTβ with an excess amount of anti-FLAG polyclonal antibody and measured newly exported surface LTβ over a 0–6-h period. Compared to the EV-expressing cells, cells expressing K3 exhibited significantly delayed kinetics of surface export (Figure 4B). In contrast, K5 expression caused little to no change in LTβ surface export (Figure 4C).

To further elucidate the alteration in LTβ trafficking induced by K3, we performed pulse-chase radioactive labeling assays using

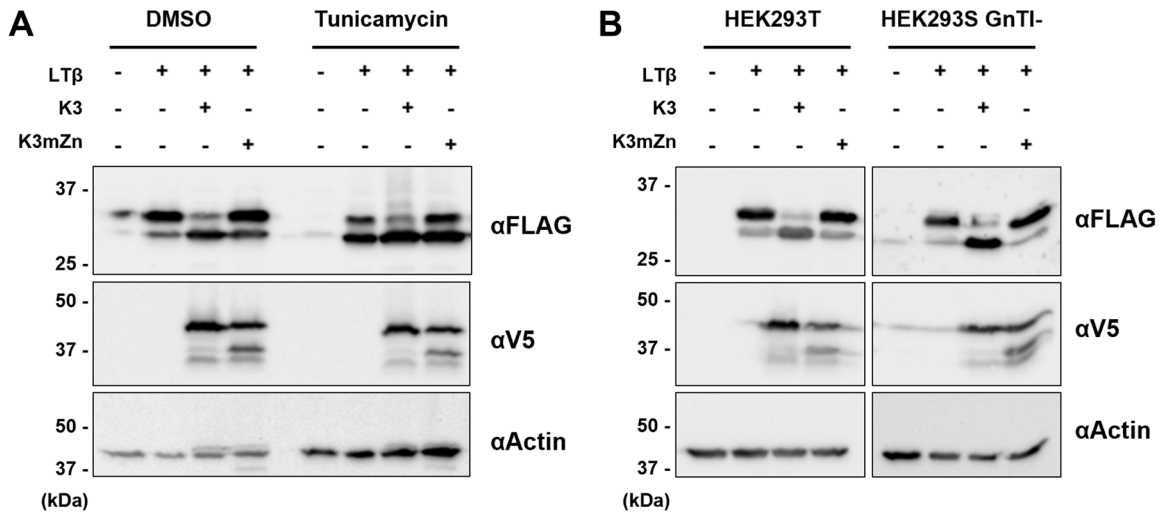

FIGURE 3 | KSHV K3 alters LTβ glycosylation. (A) The HEK293T cells were co-transfected with V5-tagged K3 or K3mZn expressing plasmids and FLAG-tagged LTβ expressing plasmids as indicated at a 1:1 ratio (1 μg each). After overnight incubation, DMSO or tunicamycin (1 μg/mL) was treated for 24 h. Cells were harvested and performed immunoblotting. (B) The HEK293T or HEK293S GnTI$^-$ cells were co-transfected with V5-tagged K3 or K5 expressing plasmids and FLAG-tagged LTβ expressing plasmids as indicated at 1:1 ratio (1 μg each). After 48 h incubation, cells were harvested and performed immunoblotting. −, empty vector transfected.

[^{35}S]methionine and [^{35}S]cysteine, followed by Endoglycosidase H (Endo H) treatment to monitor the complex glycosylation status of newly synthesized protein. In the absence of Endo H treatment, K3-expressing cells displayed a slower increase in HMW glycosylated LTβ protein levels compared to vector-expressing cells, along with a higher proportion of LMW non-glycosylated protein (Figure 4D,E). Upon Endo H treatment, LTβ failed to acquire Endo H resistance in K3-expressing cells, while vector-expressing cells showed an increase in Endo H-resistant, glycosylated LTβ over time (Figure 4D,F). Typically, glycoproteins acquire Endo H resistance after gaining complex sugar chains in the *trans*-Golgi network (TGN) [65], with GnTI enzyme acting at the *cis*-Golgi on glycan branching and elongation [61]. These findings suggest that K3 inhibits LTβ glycosylation in the early stages, thereby impeding LTβ trafficking to the cell surface membrane.

3.5 | LTβ Is Sequestered Within the ER by KSHV K3

N-glycosylation is initiated by oligosaccharyl transferase (OST) complexes in the ER, which transfer an oligosaccharide from the substrate to asparagine residues [66]. To test whether KSHV K3 co-localizes with LTβ in the ER, we examined the subcellular localization of LTβ and K3 in HeLa cells using confocal microscopy. Since LTβ is expressed on the cell surface as part of an $LT\alpha_1\beta_2$ trimer, we co-introduced LTα and LTβ into the cells and assessed the localization of LTβ with or without K3 expression. Cells were also stained with an ER-selective dye to visualize the ER compartment. Co-expression of K3 changed the intracellular distribution of LTβ, causing it to become sequestered in the ER region, whereas without K3, LTβ was scattered throughout the cytoplasm (Figure 5). In contrast, LTβ sequestration in ER region was not detected when the K3mZn mutant was co-expressed (Figure 5). These findings show that LTβ and K3 co-localize in the perinuclear region corresponding to the ER, suggesting that KSHV K3 interacts with LTβ in the ER, leading to the inhibition of LTβ glycosylation and its surface trafficking.

3.6 | The K3-Mediated Downregulation of LTβ Surface Expression Suppresses $LT\alpha_1\beta_2$–LTβR Signaling Pathway

Since $LT\alpha_1\beta_2$ is a heterotrimeric protein consisting of a soluble LTα subunit tethered to the TM protein LTβ, the surface-binding level of LTα reflects the surface expression of LTβ. Both lymphotoxins are tightly regulated inducible genes and TPA, a commonly used phorbol ester, acts as a broad-range lymphocyte activator and can induce surface expression of $LT\alpha_1\beta_2$ in both B and T cells [57, 67]. To test the effect of K3 on the surface expression of endogenous LTβ, we measured the LTα surface-binding activity on TPA-stimulated BJAB B cells with or without K3 expression. This showed that LTα surface-binding levels readily increased on TPA-stimulated BJAB-EV cells compared with the DMSO-treated control cells, whereas K3 expression markedly reduced LTα surface-binding under the same conditions (Figure 6A).

The activation of nuclear factor-κB (NF-κB) via the $LT\alpha_1\beta_2$–LTβR interaction induces the expression of various chemokines such as CCL19 (ELC), CCL21 (SLC), CXCL12 (SDF-1α), and CXCL13, which are important for initiating antiviral responses [68, 69]. To test whether K3 expression disrupts $LT\alpha_1\beta_2$–LTβR-mediated signaling pathways, we utilized TPA-activated BJAB and THP-1 cells, which express the ligand ($LT\alpha_1\beta_2$) and the receptor (LTβR), respectively (Figure 6B). We measured the phosphorylation levels of activated IκB kinases (IKKs; IKKα and β), which are key elements of the NF-κB signaling cascade. The intracellular levels of the phosphorylated IKKα/β (pIKKα/β) detectably increased in THP-1 cells co-cultured with TPA-activated BJAB-EV cells, whereas the

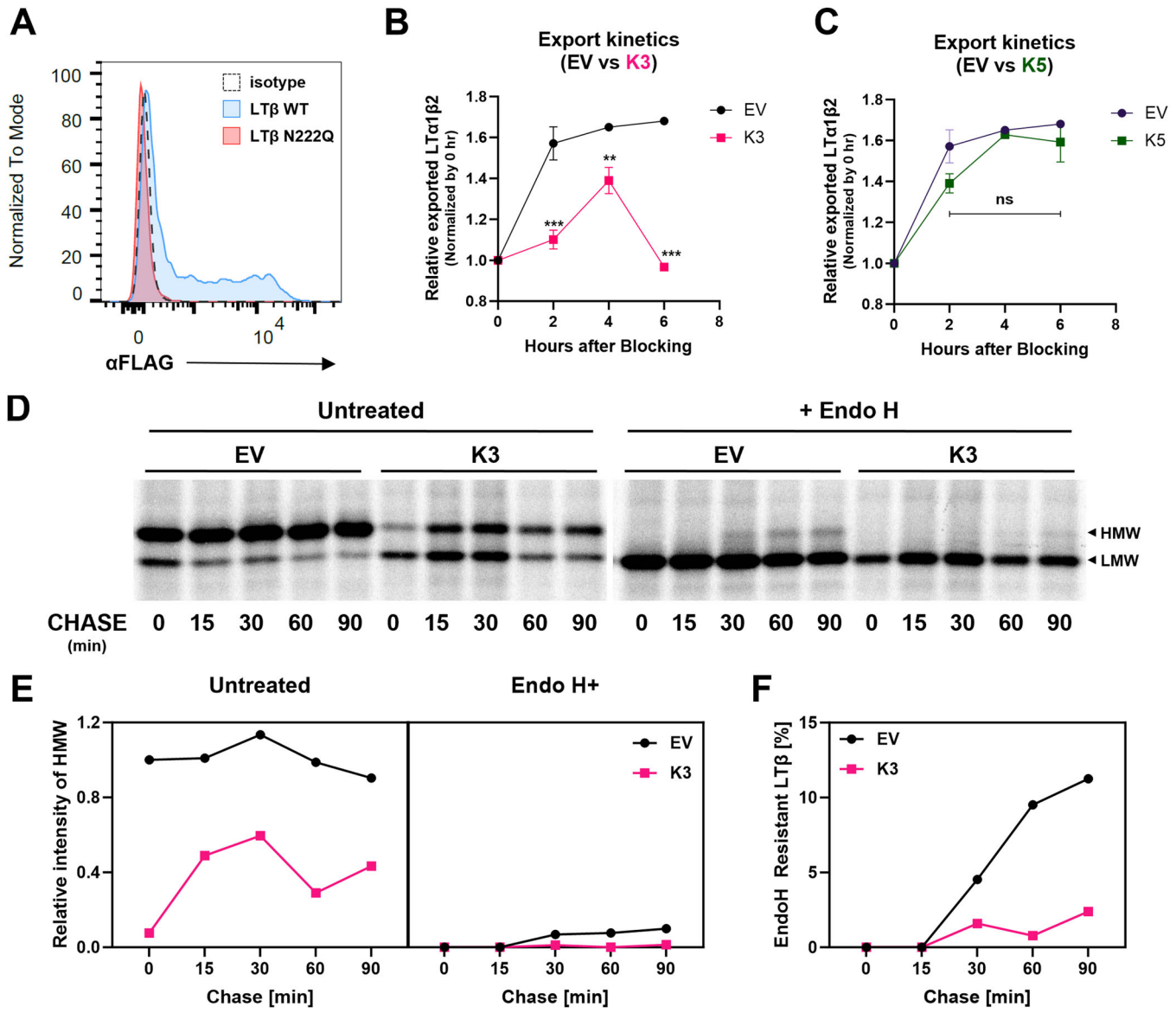

FIGURE 4 | KSHV K3 inhibits LTβ trafficking to plasma membrane. (A) The HEK293T cells were transfected with FLAG-tagged wild-type or N222Q mutant LTβ expressing plasmid. After 48 h, surface expression level of targets were stained with PE anti-FLAG antibody and measured by flow cytometry. Isotype control staining was used as a negative control. The histogram graph was presented as normalized to the mode for comparison. (B and C) Export kinetic measured from the empty vector (EV), K3 or K5-expressing BJAB stable cells. Each stable cells were transduced with LTβ-FLAG lentivirus and LTβ export kinetics were evaluated at the indicated time point. Surface expression levels of LTβ were normalized by 0 h result and presented in the graph. (D) Pulse-chase assay using EV or K3 stably expressing BJAB cell. [^{35}S] pre-labeled cells were chased for 0, 15, 30, 60, and 90 min with or without Endo H treatment. Harvested samples were immunoprecipitated with αFLAG antibody using A/G beads. (E and F) The relative intensity of HMW LTβ (E) and the ratio of EndoH-resistance LTβ in total LTβ expression (F) from (D). Signal intensity was analyzed using ImageJ/Fiji. Error bars indicate SEM from triplicates. Statistical significance was calculated using an unpaired, two-tailed Student's *t* test. ns, not significant; HMW, high molecular weight; LMW, low molecular weight; $^{**}p < 0.01$; $^{***}p < 0.001$.

induction was significantly diminished in THP-1 co-cultured with TPA-activated BJAB-K3 (Figure 6C). To further delineate this signal transduction, we pretreated TPA-activated BJAB cells with LTβR-Fc soluble protein to block the interaction between $LT\alpha_1\beta_2$ and LTβR before co-culture. This pretreatment significantly reduced pIKKα/β induction (Figure 6C), indicating that the $LT\alpha_1\beta_2$–LTβR interaction significantly induces NF-κB activation in these conditions.

To further evaluate the downstream signal activity of LTβR, we isolated THP-1 cells by removing TPA-activated BJAB cells using mouse anti-CD19 antibody and anti-mouse IgG microbeads after co-culture, and then measured the transcriptional changes of *CCL19* and *CXCL12*. The expression of these chemokines was significantly induced in THP-1 cells co-cultured with TPA-activated BJAB-EV cells, whereas their induction was markedly reduced in THP-1 cells co-cultured with TPA-activated BJAB-K3 cells (Figure 6D). Furthermore, pretreatment with LTβR-Fc attenuated chemokine induction (Figure 6D). Collectively, these data demonstrate that K3 downregulates LTβ surface expression, impairing $LT\alpha_1\beta_2$–LTβ-mediated downstream signaling pathways.

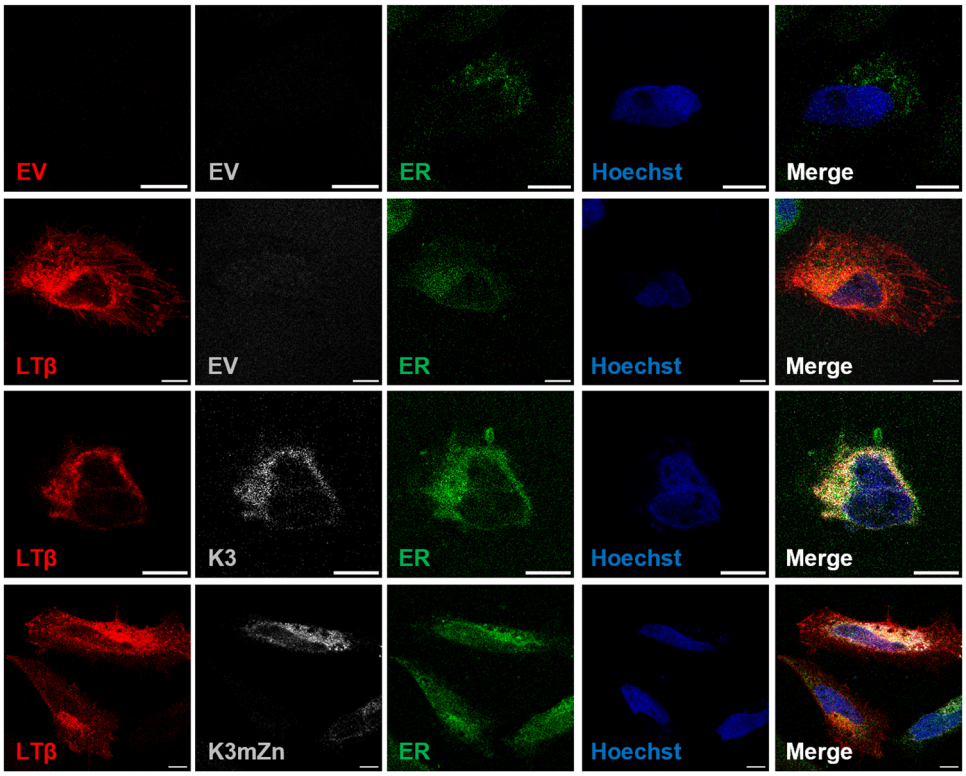

FIGURE 5 | LTβ is sequestered within the ER by KSHV K3. HeLa cells were transfected with K3/K3mZn-miRFP670nano3 expressing plasmids, and LTβ-mScarlet-I-T2A-LTα expressing plasmid, and empty vectors corresponding to each as indicated (total 2 μg). At 18 h post-transfection, cells were stained with an ER-selective dye following the manufacture's instruction and fixed with 4% PFA. Scale bar = 10 μm.

3.7 | K3 Alters the Surface Expression and Modification Status of LTβ During De Novo KSHV Infection

To examine whether K3-mediated regulation of LTβ occurs under viral infection conditions, we assessed changes in LTβ expression following de novo KSHV infection using KSHV BAC16 WT or the K3-deleted mutant (ΔK3) virus [54]. We infected HEK293T cells overexpressing LTβ with either KSHV BAC16 WT or the ΔK3 virus and analyzed LTβ surface expression and glycosylation status (Figure 7). Compared to the mock control, KSHV BAC16 WT infection led to a significant reduction in LTβ surface expression, whereas the ΔK3 mutant virus showed a markedly reduced ability to suppress LTβ surface expression (Figure 7A). In addition to changes in surface expression, we observed differences in the glycosylation pattern of LTβ. Upon KSHV BAC16 WT infection, a lower molecular weight form of LTβ, indicative of unglycosylation, was detected. This smaller LTβ form was not observed under uninfected conditions (Figure 7B). Notably, unglycosylated LTβ was also absent when cells were infected with the ΔK3 mutant virus (Figure 7B). These findings are consistent with our previous observations from overexpression systems (Figure 7B). These findings demonstrate that K3 effectively downregulates LTβ surface expression and alters its modification status in the context of viral infection.

4 | Discussion

The critical role of K3 and K5 in immune evasion through the downregulation and degradation of various target proteins has been extensively studied [70]. These regulations facilitate viral replication and persistence in the infected host cell. In this study, we identified LTβ as a new shared target of K3 and K5. Our results demonstrate that the surface expression of LTβ, which forms a membrane-bound heterotrimer with LTα, is downregulated by K3 and K5. An intriguing aspect of our findings is the novel regulatory mechanism by which K3 interferes with LTβ surface expression, by disrupting N-glycosylation and ultimately inhibiting its export trafficking in both ectopic expression of K3 and virus de novo infection condition.

Throughout our experiments, the expression of LTβ consistently showed a smaller, immature form when co-expressed with K3. Further validation revealed this as unglycosylated form of LTβ (Figures 1B and 2A). LTβ has a single glycosylation residue at N222, which is critical for its trafficking to the plasma membrane and heterotrimerization with LTα [57, 63, 64]. Due to this immature glycosylation, LTβ appeared to be trapped in ER region and failed to be transported to the plasma membrane (Figures 4B and 5B). Interestingly, this glycosylation defect is correlated with the E3 ligase enzymatic function of the RING-CH domain of K3 (Figure 1A). KSHV K3 and K5 have been reported to attach ubiquitin moieties to Lys (K), Ser (S), Thr (T), and/or Cys (C) residues [38–40]. The 30-amino-acid cytoplasmic region of LTβ has only a single serine residue (S10) and no lysine, threonine or cysteine residues. Interestingly, surface expression of the LTβ S10A mutant was still downregulated by K3 (data not shown). These results indicate that the defects in glycosylation and surface expression of LTβ are dependent on K3 E3 ligase function, whereas LTβ itself may not be directly ubiquitinated by K3.

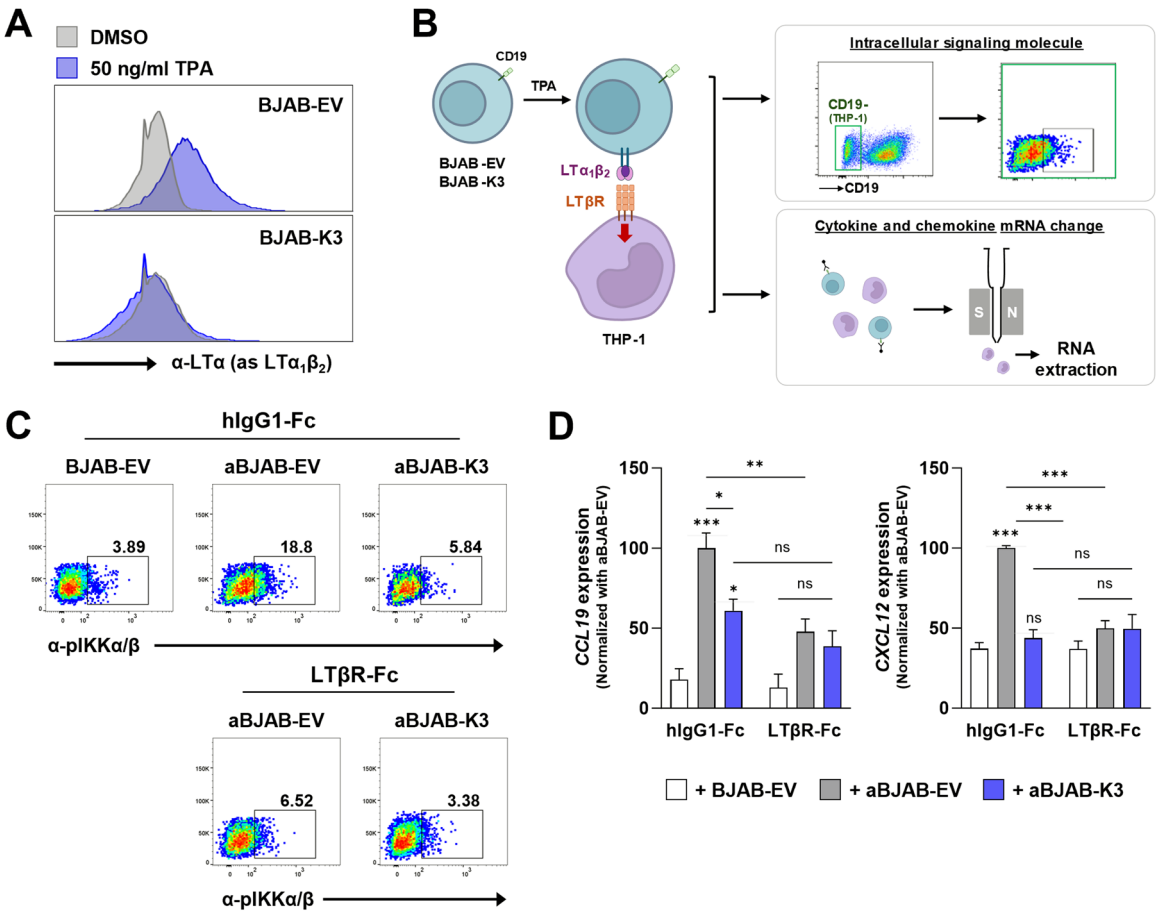

FIGURE 6 | Downregulated LTβ by KSHV K3 alters the LTβR downstream signaling pathway. (A) BJAB-empty vector (EV) and BJAB-K3 stable cell lines were stimulated with 12-O-Tetradecanoylphorbol-13-acetate (TPA) for 48 h and surface expression of LTα was measured by flow cytometry. (B) The schematic diagram for the co-culture system. THP-1 cells were stimulated with BJAB-EV, activated BJAB-EV (aBJAB-EV), or activated BJAB-K3 (aBJAB-K3) for 16 h. (C) Co-cultured cells were fixed and permeabilization was followed by PE anti-CD19 antibody and then intracellular staining was performed with anti α-pIKKα/β. Within CD19-negative cells (THP-1 cells), pIKKα/β population is presented. (D) From co-cultured cells, THP-1 cells were negatively separated, and further qRT-PCR was performed. Error bars indicate SEM from duplicates. Statistical significance was calculated using an unpaired, two-tailed Student's *t* test. ns, not significant; $*p < 0.05$; $**p < 0.01$; $***p < 0.001$.

The mechanism by which K3 inhibits the glycosylation of LTβ is not entirely understood. Based on the observation that K3 directly interacts with the immature form of LTβ (Figure 2A), it is speculated that K3 may interfere with the capacity of the enzymes involved in LTβ glycosylation or maturation. A similar mode of action has been suggested for MARCH8, a human homolog of the MARCH proteins. Human MARCH8 has been reported to inhibit the glycosylation maturation of Ebola virus glycoprotein, SARS-CoV-2 spike protein, and influenza A virus HA protein, trapping them in intracellular compartments [71–73]. This inhibition by MARCH8 is thought to occur through its binding to both the target proteins and the cellular proprotein convertase, furin, which plays a role in the maturation of viral proteins. Consequently, MARCH8 inhibits the cleavage and glycosylation maturation of viral proteins by furin, leading to their retention within the cell [72]. Similarly, it could be plausible that KSHV K3 interferes with the function of an unknown protein(s) involved in the maturation and glycosylation of LTβ, thereby causing the retention of LTβ in intracellular compartments (Figure 5B). Further in-depth research is needed to identify the specific cellular components responsible for this regulation.

Our findings indicate that the downregulation of LTβ surface expression limits the LTβR signaling pathway mediated by $LT\alpha_1\beta_2$–LTβR interaction. K3 expression in BJAB cells reduced $LT\alpha_1\beta_2$ surface expression, leading to decreased LTβR downstream signaling in THP-1 cells (Figure 6). In various viral infection models, the LTα1β2–LTβR-IFN axis has been shown to play a critical role [46, 48, 74, 75]. For example, during murine cytomegalovirus (MCMV) infection, $LT\alpha_1\beta_2$–LTβR signaling indirectly induces IFNβ within 8 h by activating monocytes, which are the primary source of IFNβ. Mice deficient in this signaling fail to control MCMV infection, showing nearly 100-fold higher viral loads [46]. Similarly, in lymphocytic choriomeningitis virus (LCMV) infection, B cell-derived $LT\alpha_1\beta_2$ is important for type I IFN induction by reorganizing lymphoid architecture [74, 75]. LTβR signaling deficient mice exhibit unorganized B-cell follicle structures in lymph nodes and lack normal splenic marginal zones, resulting in the production of only about 3% of wild-type levels of type I IFN. The indirect induction of IFN via LTβR signaling involves B cells expressing $LT\alpha_1\beta_2$, which activate LTβR on monocytes, creating an immune environment to induce IFNβ production [46, 48, 74]. In this context, KSHV, which establishes a lifelong infection in

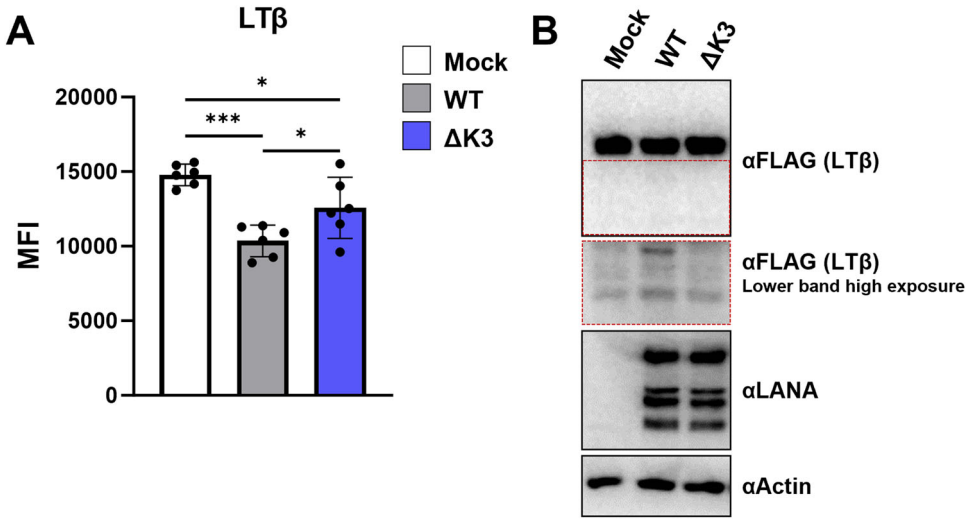

FIGURE 7 | De novo KSHV infection regulates LTβ surface expression and glycosylation. (A) FLAG-tagged LTβ-overexpressing HEK293T cells were infected with KSHV BAC16 WT or ΔK3 at MOI 1. At 48 hpi, cells were harvested and fixed with 4% PFA. The surface expression level of LTβ was measured by using APC anti-FLAG labeling in total cells (mock) or virus-positive cell (GFP+, WT, and ΔK3). (B) LTβ-overexpressing HEK293T cells were infected with KSHV BAC16 WT or ΔK3 at MOI 1. At 48 hpi, cells were harvested and performed immunoblotting. Error bars indicate SEM from two sets of triplicates. Statistical significance was calculated using an unpaired, two-tailed Student's *t* test. $*p < 0.05$; $***p < 0.001$.

B cells [76, 77], a crucial source of $LT\alpha_1\beta_2$, may evade the early IFN-mediated antiviral response by reducing LTβ surface expression on infected B cells. This suppression of LTβR signaling potentially weakens the IFN response, a well-characterized immune evasion strategy employed by KSHV during both de novo infection and reactivation [78, 79].

In addition to antiviral responses by type I IFN induction, another well-known function of $LT\alpha_1\beta_2$–LTβR interaction is the maintenance of lymphoid microenvironment [80, 81]. The $LT\alpha_1\beta_2$-dependent LTβR signaling pathway helps to establish proper lymphoid organ structures in spleen and lymph nodes, including germinal center and reticular network formation in spleen [82–86] and high endothelial venule structure in the lymph node [87]. In mouse models, the absence of secondary lymphoid tissues due to defective LTβR signaling leads to splenomegaly and an increased lymphocyte count in non-lymphoid tissues. From a pathogenic perspective, KSHV can cause several conditions that affect the secondary lymphoid organs, including lymph node KS, MCD, and lymphoma [1–3]. Although K3 and K5 are lytic genes, they have been reported to be expressed in latently infected B cells independently of the lytic cycle activation [33]. Based on our results, it is possible that alterations in LTβR signaling regulated by K3 and K5 may affect not only IFN-mediated antiviral functions but also further pathogenic processes by disrupting lymphoid organ homeostasis and normal microenvironment. Despite the potential roles K3 may play, from viral infection to the structural organization of immune organs by regulating LTβ expression, the main challenge in validating these possibilities is the complexity of the $LT\alpha_1\beta_2$–LTβR signaling axis. This pathway involves recruiting various cell types to the vicinity of signal-initiating cells, leading to their activation and contributing to the formation of higher-order immune structures [85]. Ultimately, these alterations induce type I IFN responses and change the organ microstructures, however, the induction is primarily indirect and confirmed only *in vivo* systems [46, 84]. Therefore, to better understand the physiological and pathological changes resulting from the K3-mediated downregulation of LTβ expression, follow-up studies using advanced models such as organoids or animal models are necessary.

In summary, our study identifies LTβ as a novel target of the viral E3 ligase proteins KSHV K3 and K5. We further demonstrate that K3 uniquely interferes with LTβ glycosylation, inhibiting its trafficking to the plasma membrane. This downregulation of LTβ surface expression impairs the LTβR signaling pathway, potentially aiding KSHV in evading early IFN-mediated antiviral responses and disrupting lymphoid organ homeostasis. These findings enhance our understanding of KSHV's immune evasion strategies and may inform future therapeutic approaches targeting viral persistence and pathogenesis.

Author Contributions

Soowon Kang: conceptualization, data curation, formal analysis, investigation, methodology, validation, visualization, writing (original draft, review, and editing). **Kevin Brulois:** conceptualization, data curation, formal analysis, investigation, methodology, validation, visualization. **Youn Jung Choi:** conceptualization, writing (review and editing). **Shaoyan Zhang:** writing (review and editing). **Jae U. Jung:** conceptualization, data curation, funding acquisition, project administration, resources, supervision, validation, writing (review and editing).

Acknowledgments

This study was supported by grants from the US *National Institutes of Health (NIH)* CA251275, CA294881, AI152190, AI17120, AI181758, DE023926, DE028521, and U01 CA294881 (Jae U. Jung) and a gift from Sheikha Fatima bint Mubarak.

Conflicts of Interest

The authors declare no conflicts of interest.

Data Availability Statement

The data that support the findings of this study are available from the corresponding author upon reasonable request.

References

1. Y. Chang, E. Cesarman, M. S. Pessin, et al., "Identification of Herpesvirus-Like DNA Sequences in AIDS-associated Kaposi's Sarcoma," *Science* 266 (1994): 1865–1869.

2. E. Cesarman, Y. Chang, P. S. Moore, J. W. Said, and D. M. Knowles, "Kaposi's Sarcoma-Associated Herpesvirus-Like DNA Sequences in AIDS-Related Body-Cavity-Based Lymphomas," *New England Journal of Medicine* 332 (1995): 1186–1191.

3. A. Gessain, A Sudaka, J Briere, et al., "Kaposi Sarcoma-associated Herpes-like Virus (Human Herpesvirus Type 8) DNA Sequences in Multicentric Castleman's Disease: Is There Any Relevant Association in Non-Human Immunodeficiency Virus-Infected Patients?," *Blood* 87 (1996): 414. –416.

4. R. Renne, M. Lagunoff, W. Zhong, and D. Ganem, "The Size and Conformation of Kaposi's Sarcoma-Associated Herpesvirus (Human Herpesvirus 8) DNA in Infected Cells and Virions," *Journal of Virology* 70 (1996): 8151–8154.

5. L. Yan, V. Majerciak, Z. M. Zheng, and K. Lan, "Towards Better Understanding of KSHV Life Cycle: From Transcription and Post-transcriptional Regulations to Pathogenesis," *Virologica Sinica* 34 (2019): 135–161.

6. H. R. Lee, K. Brulois, L. Wong, and J. U. Jung, "Modulation of Immune System by Kaposi's Sarcoma-Associated Herpesvirus: Lessons from Viral Evasion Strategies," *Frontiers in Microbiology* 3 (2012): 44.

7. F. Meyer, E. Ehlers, A. Steadman, T. Waterbury, M. Cao, and L. Zhang, "TLR-TRIF Pathway Enhances the Expression of KSHV Replication and Transcription Activator," *Journal of Biological Chemistry* 288 (2013): 20435–20442.

8. A. Lingel, E. Ehlers, Q. Wang, et al., "Kaposi's Sarcoma-Associated Herpesvirus Reduces Cellular Myeloid Differentiation Primary-Response Gene 88 (MyD88) Expression via Modulation of Its RNA," *Journal of Virology* 90 (2016): 180–188.

9. K. A. Bussey, E. Reimer, H. Todt, et al., "The Gammaherpesviruses Kaposi's Sarcoma-Associated Herpesvirus and Murine Gammaherpesvirus 68 Modulate the Toll-Like Receptor-Induced Proinflammatory Cytokine Response," *Journal of Virology* 88 (2014): 9245–9259.

10. J. Nicholas, "Human Herpesvirus 8-encoded Proteins With Potential Roles in Virus-Associated Neoplasia," *Frontiers in Bioscience* 12 (2007): 265–281.

11. C. Bais, A. Van Geelen, P. Eroles, et al., "Kaposi's Sarcoma Associated Herpesvirus G Protein-Coupled Receptor Immortalizes Human Endothelial Cells by Activation of the VEGF Receptor-2/KDR," *Cancer Cell* 3 (2003): 131–143.

12. A. Sodhi, S. Montaner, V. Patel, et al., "The Kaposi's Sarcoma-Associated Herpes Virus G Protein-Coupled Receptor Up-Regulates Vascular Endothelial Growth Factor Expression and Secretion Through Mitogen-Activated Protein Kinase and p38 Pathways Acting on Hypoxia-Inducible Factor 1Alpha," *Cancer Research* 60 (2000): 4873–4880.

13. M. Cannon, "The KSHV and Other Human Herpesviral G Protein-Coupled Receptors," *Current Topics in Microbiology and Immunology* 312 (2007): 137–156.

14. V. Bottero, N. Kerur, S. Sadagopan, K. Patel, N. Sharma-Walia, and B. Chandran, "Phosphorylation and Polyubiquitination of Transforming Growth Factor β-Activated Kinase 1 Are Necessary for Activation of NF-κB by the Kaposi's Sarcoma-Associated Herpesvirus G Protein-Coupled Receptor," *Journal of Virology* 85 (2011): 1980–1993.

15. M. Cannon, N. J. Philpott, and E. Cesarman, "The Kaposi's Sarcoma-Associated Herpesvirus G Protein-Coupled Receptor Has Broad Signaling Effects in Primary Effusion Lymphoma Cells," *Journal of Virology* 77 (2003): 57–67.

16. M. L. Cannon and E. Cesarman, "The KSHV G Protein-Coupled Receptor Signals via Multiple Pathways to Induce Transcription Factor Activation in Primary Effusion Lymphoma Cells," *Oncogene* 23 (2004): 514–523.

17. B. Abere, T. M. Mamo, S. Hartmann, et al., "The Kaposi's Sarcoma-Associated Herpesvirus (KSHV) Non-Structural Membrane Protein K15 Is Required for Viral Lytic Replication and May Represent a Therapeutic Target," *PLoS Pathogens* 13 (2017): e1006639.

18. L. Steinbrück, M. Gustems, S. Medele, T. F. Schulz, D. Lutter, and W. Hammerschmidt, "K1 and K15 of Kaposi's Sarcoma-Associated Herpesvirus Are Partial Functional Homologues of Latent Membrane Protein 2A of Epstein-Barr Virus," *Journal of Virology* 89 (2015): 7248–7261.

19. P. M. Anders, Z. Zhang, P. M. Bhende, L. Giffin, and B. Damania, "The KSHV K1 Protein Modulates AMPK Function to Enhance Cell Survival," *PLoS Pathogens* 12 (2016): e1005985.

20. B. Abere, N. Samarina, S. Gramolelli, et al., "Kaposi's Sarcoma-Associated Herpesvirus Nonstructural Membrane Protein pK15 Recruits the Class II Phosphatidylinositol 3-Kinase PI3K-C2α To Activate Productive Viral Replication," *Journal of Virology* 92 (2018): e00544-18.

21. J. M. Boname and P. J. Lehner, "What Has the Study of the K3 and K5 Viral Ubiquitin E3 Ligases Taught Us About Ubiquitin-Mediated Receptor Regulation?," *Viruses* 3 (2011): 118–131.

22. J. M. Boname and P. G. Stevenson, "Mhc Class I Ubiquitination by a Viral PHD/LAP Finger Protein," *Immunity* 15 (2001): 627–636.

23. S. Ishido, J. K. Choi, B. S. Lee, et al., "Inhibition of Natural Killer Cell-Mediated Cytotoxicity by Kaposi's Sarcoma-Associated Herpesvirus K5 Protein," *Immunity* 13 (2000): 365–374.

24. L. Coscoy and D. Ganem, "A Viral Protein That Selectively Downregulates ICAM-1 and B7-2 and Modulates T Cell Costimulation," *Journal of Clinical Investigation* 107 (2001): 1599–1606.

25. E. W. Hewitt, et al., "Ubiquitylation of MHC Class I by the K3 Viral Protein Signals Internalization and TSG101-dependent Degradation," *EMBO Journal* 21 (2002): 2418–2429.

26. S. M. Lang, M. O. F. Bynoe, R. Karki, M. A. Tartell, and R. E. Means, "Kaposi's Sarcoma-Associated Herpesvirus K3 and K5 Proteins Down Regulate Both DC-SIGN and DC-SIGNR," *PLoS One* 8 (2013): e58056.

27. D. J. Sanchez, J. E. Gumperz, and D. Ganem, "Regulation of CD1d Expression and Function by a Herpesvirus Infection," *Journal of Clinical Investigation* 115 (2005): 1369–1378.

28. M. Haque, J. Chen, K. Ueda, et al., "Identification and Analysis of the K5 Gene of Kaposi's Sarcoma-Associated Herpesvirus," *Journal of Virology* 74 (2000): 2867–2875.

29. P. Rimessi, A. Bonaccorsi, M. Stürzl, et al., "Transcription Pattern of Human Herpesvirus 8 Open Reading Frame K3 in Primary Effusion Lymphoma and Kaposi's Sarcoma," *Journal of Virology* 75 (2001): 7161–7174.

30. J. L. Taylor, H. N. Bennett, B. A. Snyder, P. S. Moore, and Y. Chang, "Transcriptional Analysis of Latent and Inducible Kaposi's Sarcoma-Associated Herpesvirus Transcripts in the K4 to K7 Region," *Journal of Virology* 79 (2005): 15099–15106.

31. R. Sun, S. F. Lin, K. Staskus, et al., "Kinetics of Kaposi's Sarcoma-Associated Herpesvirus Gene Expression," *Journal of Virology* 73 (1999): 2232–2242.

32. F. X. Zhu, T. Cusano, and Y. Yuan, "Identification of the Immediate-Early Transcripts of Kaposi's Sarcoma-Associated Herpesvirus," *Journal of Virology* 73 (1999): 5556–5567.

33. H. Chang, D. P. Dittmer, S. Y. Chul, Y. Hong, and J. U. Jung, "Role of Notch Signal Transduction in Kaposi's Sarcoma-Associated Herpesvirus Gene Expression," *Journal of Virology* 79 (2005): 14371–14382.

34. R. E. Means, "Multiple Endocytic Trafficking Pathways of MHC Class I Molecules Induced by a Herpesvirus Protein," *EMBO Journal* 21 (2002): 1638–1649.

35. R. B. Dodd, M. D. Allen, S. E. Brown, et al., "Solution Structure of the Kaposi's Sarcoma-Associated Herpesvirus K3 N-Terminal Domain Reveals a Novel E2-Binding C4HC3-Type RING Domain," *Journal of Biological Chemistry* 279 (2004): 53840–53847.

36. L. Coscoy, D. J. Sanchez, and D. Ganem, "A Novel Class of Herpesvirus-Encoded Membrane-Bound E3 Ubiquitin Ligases Regulates Endocytosis of Proteins Involved in Immune Recognition," *Journal of Cell Biology* 155 (2001): 1265–1274.

37. M. Ohmura-Hoshino, E. Goto, Y. Matsuki, et al., "A Novel Family of Membrane-Bound E3 Ubiquitin Ligases," *Journal of Biochemistry* 140 (2006): 147–154.

38. K. Cadwell and L. Coscoy, "The Specificities of Kaposi's Sarcoma-Associated Herpesvirus-Encoded E3 Ubiquitin Ligases Are Determined by the Positions of Lysine or Cysteine Residues Within the Intracytoplasmic Domains of Their Targets," *Journal of Virology* 82 (2008): 4184–4189.

39. K. Cadwell and L. Coscoy, "Ubiquitination on Nonlysine Residues by a Viral E3 Ubiquitin Ligase," *Science* 309 (2005): 127–130.

40. X. Wang, R. A. Herr, W. J. Chua, L. Lybarger, E. Wiertz, and T. H. Hansen, "Ubiquitination of Serine, Threonine, or Lysine Residues on the Cytoplasmic Tail Can Induce ERAD of MHC-I by Viral E3 Ligase mK3," *Journal of Cell Biology* 177 (2007): 613–624.

41. J. L. Browning, M. J. Androlewicz, and C. F. Ware, "Lymphotoxin and an Associated 33-kDa Glycoprotein Are Expressed on the Surface of an Activated Human T Cell Hybridoma," *Journal of Immunology* 147 (1991): 1230–1237.

42. M. J. Androlewicz, J. L. Browning, and C. F. Ware, "Lymphotoxin Is Expressed As a Heteromeric Complex With a Distinct 33-kDa Glycoprotein on the Surface of an Activated Human T Cell Hybridoma," *Journal of Biological Chemistry* 267 (1992): 2542–2547.

43. D. N. Mauri, R. Ebner, R. I. Montgomery, et al., "LIGHT, a New Member of the TNF Superfamily, and Lymphotoxin α Are Ligands for Herpesvirus Entry Mediator," *Immunity* 8 (1998): 21–30.

44. C. A. Benedict, T. A. Banks, L. Senderowicz, et al., "Lymphotoxins and Cytomegalovirus Cooperatively Induce Interferon-β, Establishing Host-Virus Détente," *Immunity* 15 (2001): 617–626.

45. A. C. Iversen, P. S. Norris, C. F. Ware, and C. A. Benedict, "Human NK Cells Inhibit Cytomegalovirus Replication Through a Noncytolytic Mechanism Involving Lymphotoxin-Dependent Induction of IFN-β," *Journal of Immunology* 175 (2005): 7568–7574.

46. T. A. Banks, S. Rickert, C. A. Benedict, et al., "A Lymphotoxin-IFN-β Axis Essential for Lymphocyte Survival Revealed during Cytomegalovirus Infection," *Journal of Immunology* 174 (2005): 7217–7225.

47. K. M. Hsu, J. R. Pratt, W. J. Akers, S. I. Achilefu, and W. M. Yokoyama, "Murine Cytomegalovirus Displays Selective Infection of Cells Within Hours After Systemic Administration," *Journal of General Virology* 90 (2009): 33–43.

48. K. Schneider, A. Loewendorf, C. De Trez, et al., "Lymphotoxin-Mediated Crosstalk Between B Cells and Splenic Stroma Promotes the Initial Type I Interferon Response to Cytomegalovirus," *Cell Host & Microbe* 3 (2008): 67–76.

49. E. A. Moseman, M. Iannacone, L. Bosurgi, et al., "B Cell Maintenance of Subcapsular Sinus Macrophages Protects Against a Fatal Viral Infection Independent of Adaptive Immunity," *Immunity* 36 (2012): 415–426.

50. N. Honke, N. Shaabani, G. Cadeddu, et al., "Enforced Viral Replication Activates Adaptive Immunity and Is Essential for the Control of a Cytopathic Virus," *Nature Immunology* 13 (2011): 51–57.

51. S. Ishido, C. Wang, B. S. Lee, G. B. Cohen, and J. U. Jung, "Downregulation of Major Histocompatibility Complex Class I Molecules by Kaposi's Sarcoma-Associated Herpesvirus K3 and K5 Proteins," *Journal of Virology* 74 (2000): 5300–5309.

52. R. E. Means, S. M. Lang, and J. U. Jung, "The Kaposi's Sarcoma-Associated Herpesvirus K5 E3 Ubiquitin Ligase Modulates Targets by Multiple Molecular Mechanisms," *Journal of Virology* 81 (2007): 6573–6583.

53. A. Hayer, L. Shao, M. Chung, et al., "Engulfed Cadherin Fingers Are Polarized Junctional Structures Between Collectively Migrating Endothelial Cells," *Nature Cell Biology* 18 (2016): 1311–1323.

54. K. F. Brulois, H. Chang, A. S. Lee, et al., "Construction and Manipulation of a New Kaposi's Sarcoma-Associated Herpesvirus Bacterial Artificial Chromosome Clone," *Journal of Virology* 86 (2012): 9708–9720.

55. J. Myoung and D. Ganem, "Generation of a Doxycycline-Inducible KSHV Producer Cell Line of Endothelial Origin: Maintenance of Tight Latency With Efficient Reactivation Upon Induction," *Journal of Virological Methods* 174 (2011): 12–21.

56. H. Gruss and S. Dower, "Tumor Necrosis Factor Ligand Superfamily: Involvement in the Pathology of Malignant Lymphomas," *Blood* 85 (1995): 3378–3404.

57. J. Browning, et al., "Lymphotoxin?, a Novel Member of the TNF Family That Forms a Heteromeric Complex With Lymphotoxin on the Cell Surface," *Cell* 72 (1993): 847–856.

58. M. Kajikawa, M. Hata, M. Ishimura, et al., "Importance of Accessibility to the Extracellular Juxtamembrane Stalk Region of Membrane Protein for Substrate Recognition by Viral Ubiquitin Ligase K5," *Biochemical Journal* 479 (2022): 2261–2278.

59. S. J. Deeb, J. Cox, M. Schmidt-Supprian, and M. Mann, "N-Linked Glycosylation Enrichment for In-Depth Cell Surface Proteomics of Diffuse Large B-Cell Lymphoma Subtypes," *Molecular & Cellular Proteomics* 13 (2014): 240–251.

60. D. Duksin and W. C. Mahoney, "Relationship of the Structure and Biological Activity of the Natural Homologues of Tunicamycin," *Journal of Biological Chemistry* 257 (1982): 3105–3109.

61. P. J. Reeves, N. Callewaert, R. Contreras, and H. G. Khorana, "Structure and Function in Rhodopsin: High-Level Expression of Rhodopsin With Restricted and Homogeneous N-Glycosylation by a Tetracycline-Inducible N-Acetylglucosaminyltransferase I-Negative HEK293S Stable Mammalian Cell Line," *Proceedings of the National Academy of Sciences* 99 (2002): 13419–13424.

62. K. T. Schjoldager, Y. Narimatsu, H. J. Joshi, and H. Clausen, "Global View of Human Protein Glycosylation Pathways and Functions," *Nature Reviews Molecular Cell Biology* 21 (2020): 729–749.

63. J. L. Browning, I. Dougas, A. Ngam-ek, et al., "Characterization of Surface Lymphotoxin Forms. Use of Specific Monoclonal Antibodies and Soluble Receptors," *Journal of Immunology* 154 (1995): 33–46.

64. J. L. Browning, K. Miatkowski, D. A. Griffiths, et al., "Preparation and Characterization of Soluble Recombinant Heterotrimeric Complexes of Human Lymphotoxins Alpha and Beta," *Journal of Biological Chemistry* 271 (1996): 8618–8626.

65. H. H. Freeze and C. Kranz, "Endoglycosidase and Glycoamidase Release of N-Linked Glycans," *Current Protocols in Molecular Biology* 17 (2010): 1–25.

66. A. Helenius and M. Aebi, "Roles of N-Linked Glycans in the Endoplasmic Reticulum," *Annual Review of Biochemistry* 73 (2004): 1019–1049.

67. A. V. Tumanov, D. V. Kuprash, M. A. Lagarkova, et al., "Distinct Role of Surface Lymphotoxin Expressed by B Cells in the Organization of Secondary Lymphoid Tissues," *Immunity* 17 (2002): 239–250.

68. E. Dejardin, N. M. Droin, M. Delhase, et al., "The Lymphotoxin-β Receptor Induces Different Patterns of Gene Expression via Two NF-κB Pathways," *Immunity* 17 (2002): 525–535.

69. C. Huber, C. Thielen, H. Seeger, et al., "Lymphotoxin-β Receptor-Dependent Genes in Lymph Node and Follicular Dendritic Cell Transcriptomes," *Journal of Immunology* 174 (2005): 5526–5536.

70. P. J. Lehner, S. Hoer, R. Dodd, and L. M. Duncan, "Downregulation of Cell Surface Receptors by the K3 Family of Viral and Cellular Ubiquitin E3 Ligases," *Immunological Reviews* 207 (2005): 112–125.

71. C. Yu, S. Li, X. Zhang, et al., "MARCH8 Inhibits Ebola Virus Glycoprotein, Human Immunodeficiency Virus Type 1 Envelope Glycoprotein, and Avian Influenza Virus H5N1 Hemagglutinin Maturation," *mBio* 11 (2020): e01882-20.

72. Y. Zhang, S. Ozono, T. Tada, et al., "MARCH8 Targets Cytoplasmic Lysine Residues of Various Viral Envelope Glycoproteins," *Microbiology Spectrum* 10 (2022): e0061821.

73. C. M. Lun, A. A. Waheed, A. Majadly, N. Powell, and E. O. Freed, "Mechanism of Viral Glycoprotein Targeting by Membrane-Associated RING-CH Proteins," *mBio* 12 (2021): e00219-21.

74. J. Louten, N. van Rooijen, and C. A. Biron, "Type 1 IFN Deficiency in the Absence of Normal Splenic Architecture During Lymphocytic Choriomeningitis Virus Infection," *Journal of Immunology* 177 (2006): 3266–3272.

75. V. Kumar, E. Scandella, R. Danuser, et al., "Global Lymphoid Tissue Remodeling during a Viral Infection Is Orchestrated by a B Cell-Lymphotoxin-Dependent Pathway," *Blood* 115 (2010): 4725–4733.

76. D. Whitby, C. Boshoff, T. Hatzioannou, et al., "Detection of Kaposi Sarcoma Associated Herpesvirus in Peripheral Blood of HIV-Infected Individuals and Progression to Kaposi's Sarcoma," *Lancet* 346 (1995): 799–802.

77. J. A. Ambroziak, D. J. Blackbourn, B. G. Herndier, et al., "Herpes-Like Sequences in HIV-Infected and Uninfected Kaposi's Sarcoma Patients," *Science* 268 (1995): 582–583.

78. N. Sathish and Y. Yuan, "Evasion and Subversion of Interferon-Mediated Antiviral Immunity by Kaposi's Sarcoma-Associated Herpesvirus: An Overview," *Journal of Virology* 85 (2011): 10934–10944.

79. G. Broussard and B. Damania, "Regulation of KSHV Latency and Lytic Reactivation," *Viruses* 12 (2020): 1034.

80. N. H. Ruddle, "Lymphoid Neo-Organogenesis: Lymphotoxin's Role in Inflammation and Development," *Immunologic Research* 19 (1999): 119–125.

81. J. L. Gommerman and J. L. Browning, "Lymphotoxin/LIGHT, Lymphoid Microenvironments and Autoimmune Disease," *Nature Reviews Immunology* 3 (2003): 642–655.

82. K. M. Ansel, V. N. Ngo, P. L. Hyman, et al., "A Chemokine-Driven Positive Feedback Loop Organizes Lymphoid Follicles," *Nature* 406 (2000): 309–314.

83. D. L. Drayton, X. Ying, J. Lee, W. Lesslauer, and N. H. Ruddle, "Ectopic LTαβ Directs Lymphoid Organ Neogenesis With Concomitant Expression of Peripheral Node Addressin and a HEV-Restricted Sulfotransferase," *Journal of Experimental Medicine* 197 (2003): 1153–1163.

84. V. N. Ngo, H. Korner, M. D. Gunn, et al., "Lymphotoxin α/β and Tumor Necrosis Factor Are Required for Stromal Cell Expression of Homing Chemokines in B and T Cell Areas of the Spleen," *Journal of Experimental Medicine* 189 (1999): 403–412.

85. F. Mackay, G. R. Majeau, P. Lawton, P. S. Hochman, and J. L. Browning, "Lymphotoxin but Not Tumor Necrosis Factor Functions to Maintain Splenic Architecture and Humoral Responsiveness in Adult Mice," *European Journal of Immunology* 27 (1997): 2033–2042.

86. R. A. Fava, E. Notidis, J. Hunt, et al., "A Role for the Lymphotoxin/LIGHT Axis in the Pathogenesis of Murine Collagen-Induced Arthritis," *Journal of Immunology* 171 (2003): 115–126.

87. A. Kratz, A. Campos-Neto, M. S. Hanson, and N. H. Ruddle, "Chronic Inflammation Caused by Lymphotoxin Is Lymphoid Neogenesis," *Journal of Experimental Medicine* 183 (1996): 1461–1472.

Supporting Information

Additional supporting information can be found online in the Supporting Information section.